Int. J. Heat Mass Transfer. Vol. 13, pp. 1101–1114. Pergamon Press 1970. Printed in Great Britain

THERMAL RESPONSE BEHAVIOR OF LAMINAR BOUNDARY LAYERS IN WEDGE FLOW

JAMES L. S. CHEN*
University of Pittsburgh, Pennsylvania, U.S.A.

and

B. T. CHAO†
University of Illinois at Urbana-Champaign, Urbana, Illinois, U.S.A.

(Received 29 September 1969 and in revised form 8 January 1970)

Abstract—The thermal response behavior of incompressible, uniform property, laminar boundary layer flows over wedges has been investigated using a technique recently proposed by Chao and Cheema. Both the surface response characteristics and details of the transient temperature fields, subsequent to a step change in either the surface temperature or surface heat flux, are obtained. Results are presented for Prandtl numbers of 0·01, 0·1, 0·72, 1·0, 10 and 100 and for wedges with $\beta = -0{\cdot}1, 0, 0{\cdot}1, 0{\cdot}2, 0{\cdot}5$ and $1{\cdot}0$, $\pi\beta$ being the wedge angle. Revealing physical insight is gained by comparing the data for small times with pure conduction transients and the steady state data with those deduced for vanishingly small Prandtl number and for large Prandtl number.

NOMENCLATURE

a, $= f''(0)$;
f, dimensionless stream function;
k, thermal conductivity;
Nu, Nusselt number, defined in (31);
p, parameter in Laplace transform;
Pr, Prandtl number;
q_w, heat flux at wall;
Re, Reynolds number, $= Ux/\nu$;
T, temperature;
t, time;
U, velocity at edge of boundary layer;
u, velocity component in x-direction;
v, velocity component in y-direction;
x, coordinate along wedge surface;
y, coordinate normal to wedge surface;
$1(t)$, Heaviside unit operator, $= 0$ for $t < 0$ and $= 1$ for $t \geqslant 0$;
$\operatorname{erfc} x$, complementary error function,

$$= \frac{2}{\sqrt{\pi}} \int_x^\infty e^{-\alpha^2} \, d\alpha;$$

$i^n \operatorname{erfc} x$, nth repeated integral of the complementary error function,

$$= \int_x^\infty i^{n-1} \operatorname{erfc} \alpha \, d\alpha, n = 1, 2, \ldots.$$

Greek symbols

β, wedge angle divided by π;
$\Gamma(n)$, gamma function, $= \int_0^\infty \alpha^{n-1} e^{-\alpha} d\alpha$;
$\Gamma_x(n)$, incomplete gamma function,

$$= \int_0^x \alpha^{n-1} e^{-\alpha} d\alpha;$$

η, dimensionless coordinate, defined in (6);
θ, dimensionless temperature, defined in (13a) or (13b);

* Assistant Professor of Mechanical Engineering, formerly graduate assistant at the University of Illinois at Urbana-Champaign.

† Professor of Mechanical Engineering and of Nuclear Engineering. (Please address all correspondence to B. T. Chao.)

κ, thermal diffusivity;
λ, a parametric function, first introduced in (21);
μ, dynamic viscosity;
ν, kinematic viscosity;
τ, dimensionless time, defined in (12).

Subscripts

s, steady state;
w, wall;
∞, free stream condition;

Also, $'$ denotes differentiation with respect to η and a superscript numeral $^{(\cdot)}$ denotes the order of differentiation.

1. INTRODUCTION

THE GENERAL problem of treating unsteady, convective heat-transfer processes between a flowing fluid and its solid bounding surface due to changing flow velocity and thermal condition is highly complicated. In this investigation, we restrict ourselves to the determination of the entire time-history of the heat-transfer process in Falkner–Skan flows subsequent to a step change in the wedge's surface temperature or heat flux. The method of analysis parallels that used in [1] with improvement introduced in the formulation and in the computation procedure. As a result, the technique is set on a *firmer* foundation. In addition to the surface response characteristics, details of the transient temperature fields are also obtained. The essential features of the solution technique are:

(a) Transformation of the energy equation in the Laplace transform variable to a suitable form for which an appropriate series solution can be constructed.
(b) The introduction of a certain function, initially unknown, into the series expansion with the consequence that the solution becomes valid for all times.

It has recently been demonstrated in one case that the mathematical accuracy of the method is quite satisfactory [2].

2. GOVERNING EQUATIONS

We consider two-dimensional, laminar, incompressible boundary layers over a wedge of included angle $\pi\beta$, placed symmetrically in a uniform main stream. The flow is steady, has a constant free stream temperature T_∞, and is of negligible dissipation. Initially, the wedge surface temperature is also T_∞. At time $t = 0$, the wedge surface undergoes a step change in temperature or in heat flux. The applied thermal disturbance is limited in that changes in fluid properties are negligible. The physical model and the coordinate system are illustrated in Fig. 1.

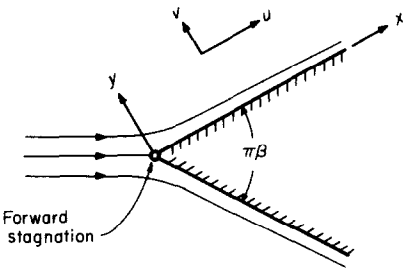

FIG. 1. Flow past a wedge. In the neighborhood of the front stagnation, the potential velocity distribution is $U(x) = Cx^m$, $m = \beta/(2-\beta)$.

The continuity and momentum equations for the stated boundary layer flow are

$$\frac{\partial u}{\partial x} + \frac{\partial v}{\partial y} = 0 \tag{1}$$

$$u\frac{\partial u}{\partial x} + v\frac{\partial u}{\partial y} = U\frac{\mathrm{d}U}{\mathrm{d}x} + \nu\frac{\partial^2 u}{\partial y^2} \tag{2}$$

where $U(x)$ is the velocity outside the boundary layer. It is well known that

$$U(x) = Cx^m \text{ with } m = \beta/(2-\beta) \text{ and } C \text{ is a constant.} \tag{3}$$

The solution of (1) and (2) under the boundary conditions

$$u(x, 0) = v(x, 0) = 0; \qquad u(x, \infty) = U(x) \tag{4}$$

is

$$u = Uf', \qquad v = -\left(\frac{m+1}{2}\frac{vU}{x}\right)^{\frac{1}{2}} \left(f - \frac{1-m}{1+m}\eta f'\right) \tag{5}$$

in which the similarity variable η is defined as

$$\eta = y\left(\frac{m+1}{2}\frac{U}{vx}\right)^{\frac{1}{2}} \tag{6}$$

and the dimensionless stream function $f(\eta)$ satisfies the Falkner–Skan equation

$$f''' + ff'' + \beta[1 - (f')^2] = 0 \tag{7}$$

with

$$f(0) = f'(0) = 0; \qquad f'(\infty) = 1. \tag{8}$$

The energy boundary-layer equation is

$$\frac{\partial T}{\partial t} + u\frac{\partial T}{\partial x} + v\frac{\partial T}{\partial y} = \kappa\frac{\partial^2 T}{\partial y^2}. \tag{9}$$

For the problem under consideration, the initial condition is

$$T(x, y, 0) = T_\infty \tag{10}$$

and the boundary conditions are:

(a) for a step change in surface temperature

$$T(x, 0, t) = T_\infty + (T_w - T_\infty)\,1(t); \qquad T(x, \infty, t) = T_\infty \tag{11a}$$

(b) for a step change in surface flux

$$\frac{\partial T}{\partial y}(x, 0, t) = -\frac{q_w}{k}\,1(t); \qquad T(x, \infty, t) = T_\infty. \tag{11b}$$

To transform the energy equation into an appropriate dimensionless form, we define

$$\tau = (m+1)\frac{Ut}{x} \tag{12}$$

and, for case (a), a dimensionless temperature

$$\theta = \frac{T - T_\infty}{T_w - T_\infty}. \tag{13a}$$

Consequently, (9) becomes

$$2Pr\left(1 - \frac{1-m}{1+m}f'\tau\right)\frac{\partial\theta}{\partial\tau} = \frac{\partial^2\theta}{\partial\eta^2} + Pr\,f\frac{\partial\theta}{\partial\eta} \tag{14}$$

with

$$\theta(\eta, 0) = 0; \qquad \theta(0, \tau) = 1(\tau), \qquad \theta(\infty, \tau) = 0. \tag{15}$$

For case (b), we define

$$\theta = \frac{T - T_\infty}{\frac{q_w}{k}\left(\frac{2}{m+1}\frac{vx}{U}\right)^{\frac{1}{2}}} \tag{13b}$$

and (9) transforms to

$$2Pr\left(1 - \frac{1-m}{1+m}f'\tau\right)\frac{\partial\theta}{\partial\tau} = \frac{\partial^2\theta}{\partial\eta^2} + Pr\left(f\frac{\partial\theta}{\partial\eta} - \frac{1-m}{1+m}f'\theta\right) \tag{16}$$

with

$$\theta(\eta, 0) = 0; \qquad \frac{\partial\theta}{\partial\eta}(0, \tau) = -1(\tau), \qquad \theta(\infty, \tau) = 0. \tag{17}$$

For stagnation flow, $m = 1$ and (14) becomes identical to (16) as expected. For flow past a flat plate, $m = 0$ and the two energy equations reduce to those given in [1].

The range of τ which is of interest here spans from 0 to ∞, and f' is a monotonically increasing function of η, starting from 0 at $\eta = 0$ and asymptotically approaches unity as $\eta \to \infty$. For boundary layers which remain attached to the wedge surface, m has the theoretical lower limit of $-0{\cdot}091$ which corresponds to $\beta = -0{\cdot}199$. Let us now consider the case $m < 1$. Subsequent to the thermal disturbance, be it a step change in temperature or in flux, there always exists a region in the boundary layer for which $\{1 - [(1-m)/(1+m)]f'\tau\} > 0$. Simultaneously, there also exists another region for which $\{\cdot\} < 0$.

When $\{\cdot\} = 0$, the equations become singular. Some means of circumventing this difficulty must be devised if a finite difference scheme of integration were used.

3. EVALUATION OF f AND ITS DERIVATIVES

To solve the energy equations, one needs the information on f. In [1], a power series solution for f (the Blasius series) was employed. Such a series has a limited radius of convergence and, thus, its use is not satisfactory for low Prandtl number fluids. In this investigation, a simple step-by-step calculation scheme was adopted, using Taylor expansion and values of $f''(0)$ reported in [3]. Highly accurate results have been obtained with very little computer time. Interested readers are referred to [4] for details. Suffice it to mention that with $\Delta\eta = 0{\cdot}01$ for $0 < \eta \leqslant 0{\cdot}1$ and $\Delta\eta = 0{\cdot}05$ for $\eta > 0{\cdot}1$ the calculated results show almost complete agreement with data listed in [5]. Deviations, when present, occurs only in the seventh digit.

4. SOLUTION METHOD AND RESULTS FOR A STEP CHANGE IN WALL TEMPERATURE

We define the Laplace transform of $\theta(\eta, \tau)$ in the usual manner, i.e.

$$\bar{\theta} = \int_0^\infty e^{-p\tau}\,\theta(\eta, \tau)\,d\tau \tag{18}$$

and obtain from (14) and (15)

$$\bar{\theta}'' + Prf\bar{\theta}' = 2Pr\left[(1-\beta)\,f'\frac{\partial(p\bar{\theta})}{\partial p} + p\bar{\theta}\right] \tag{19}$$

with

$$\bar{\theta}(0) = p^{-1}, \qquad \bar{\theta}(\infty) = 0. \tag{20}$$

By following the procedure expounded in [1, 2]*, it may be established that an appropriate series solution for (19) and (20) is

$$\bar{\theta} = p^{-1}\exp\left\{-\frac{Pr}{2}[F - (1-\beta)(\eta f - F)] - [2Pr(p+\lambda)]^{\frac{1}{2}}\eta\right\} \sum_{n=0}^{\infty} u_n(\eta)[2Pr(p+\lambda)]^{-n/2} \tag{21}$$

in which $F \equiv \int_0^\eta f\,d\eta$, $Re(p) > 0$ and λ is a real function of η, always positive, yet unknown. We set $u_0 \equiv 1$ and $u_1(0) = u_2(0) = \ldots = u_n(0) = \ldots = 0$; hence, $\bar{\theta}(0) = p^{-1}$. We shall later demonstrate that $\bar{\theta}(\infty) = 0$.

Upon substituting (21) into (19) and equating the coefficients of like powers of $(p + \lambda)$, we find

$$\begin{aligned} u_n' = {} & \frac{1}{2}u_{n-1}'' + \frac{Pr}{2}(1-\beta)\,\eta f' u_{n-1}' \\ & - Pr\eta\lambda' u_{n-2}' - (n-3)\,Pr\lambda' u_{n-3}' \\ & + \frac{Pr}{4}\Big\{(1-\beta)\,[\eta f'' + (2n-1)f'] - f' \\ & + \frac{Pr}{2}[(1-\beta)^2\eta^2(f')^2 - f^2] \\ & + 4(\eta\lambda')'\Big\}u_{n-1} + \frac{Pr}{2}[(2n-5)\,\lambda' \\ & - (\eta\lambda')' - (1-\beta)\,Prf'(\eta^2\lambda)']\,u_{n-2} \\ & + \frac{Pr}{2}\{Pr\,(\eta\lambda')^2 - (n-3)\,[\lambda'' + (1-\beta) \\ & \times Prf'(\eta\lambda' + 2\lambda)]\}\,u_{n-3} \\ & + (n - \tfrac{7}{2})\,Pr^2\eta(\lambda')^2\,u_{n-4} + \tfrac{1}{2}(n-3) \\ & \qquad (n-5)\,Pr^2(\lambda')^2\,u_{n-5} \end{aligned} \tag{22}$$

for $n \geqslant 1$ and $u_{-1} = u_{-2} = u_{-3} = u_{-4} = 0$.

The recurrent relation (22) can be integrated in succession, beginning with $n = 1$ and using the previously chosen boundary conditions. The results are

$$\begin{aligned} u_0 &\equiv 1 \\ u_1 &= X_1 + Pr\eta\lambda \\ u_2 &= X_2 + Pr\eta X_1\lambda + \tfrac{1}{2}Pr^2\eta^2\lambda^2 \end{aligned}$$

* The formulation in [1] is not the most convenient; it has since been modified although the basic idea remains intact.

etc. where

$$X_1 = \tfrac{1}{4} Pr[(1-\beta)\eta f' - f] + \tfrac{1}{8} Pr^2 \int_0^\eta [(1-\beta)^2\eta^2(f')^2 - f^2]\, d\eta$$

$$X_2 = \tfrac{1}{2}(X_1^2 + X_1') + \tfrac{1}{2} Pr(1-\beta) \times [fX_1 + \int_0^\eta (\eta f' - f)X_1'\, d\eta] \qquad (23)^*$$

etc.

With the exception of u_0 which is identically unity, each u_n consists of two parts—one is free of λ and is designated as X_n in (23); the other is a polynomial of λ. From the well known results $f''(0) = a$, $f^{(3)}(0) = -\beta$, $f^{(4)}(0) = 0$, etc., a simple calculation shows that $X_1(0) = X_2(0) = \ldots = 0$ and $X_1'(0) = 0$, $X_2'(0) = \frac{1}{8} aPr(1-2\beta)$, $X_3'(0) = -\frac{1}{16} Pr\beta(2-3\beta)$, $X_4'(0) = 0$, etc. To determine the X_n's, a step-by-step computation scheme completely analogous to that for evaluating f was used. The calculation began with X_1 and the step sizes were the same as those used for f.

The desired transient temperature field is obtained from taking the inverse of (21), using the familiar translation and convolution theorems. The result is

$$\theta(\eta, \tau) = \exp\left\{-\frac{Pr}{2}[F - (1-\beta)(\eta f - F)] - (2Pr\lambda)^{\frac{1}{2}}\eta\right\} \sum_{n=0}^{\infty} u_n (2Pr\lambda)^{-n/2} G_n \qquad (24)$$

in which

For $n \geqslant 2$, the G_n's are given by the following integral

$$G_n = 2^{n-2}\{\exp[(2Pr\lambda)^{\frac{1}{2}}\eta]\} \int_0^{\lambda\tau} z^{(n/2)-1} e^{-z} i^{n-2} \operatorname{erfc}[\tfrac{1}{2}(2Pr\lambda)^{\frac{1}{2}} z^{-\frac{1}{2}}\eta]\, dz \qquad (26)$$

and, as it turned out, they are all expressible in terms of the four g-functions. Furthermore, it can be demonstrated that

(i) G_n ranges from 0 to 1 for the entire domain of interest, namely, $0 < \tau < \infty$ and $0 < \eta < \infty$, and

(ii) $\lim_{\tau \to \infty} G_n = 1$ for all η's.

Our experience indicates that the foregoing general behavior of the G_n function is inherent with the method of analysis and is by no means unique to the present problem. This fortunate situation enhances the usefulness of the method.

The steady state temperature distribution follows from letting $\tau \to \infty$ in (24). It is

$$\theta_s(\eta) = \exp\left\{-\frac{Pr}{2}[F - (1-\beta)(\eta f - F)] - (2Pr\lambda)^{\frac{1}{2}}\eta\right\} \sum_{n=0}^{\infty} u_n (2Pr\lambda)^{-n/2}. \qquad (27)$$

By comparing (27) with (21), we conclude that $\bar{\theta}(\infty) = 0$, since $\theta_s(\infty) = 0$ and $Re(p) > 0$. Thus, an earlier expectation is realized.

Differentiating (24) with respect to η and evaluating the result for $\eta = 0$ yield

$$-\theta'(0, \tau) = (2Pr)^{\frac{1}{2}}(\pi\tau)^{-\frac{1}{2}} \exp(-\lambda\tau) + (2Pr\lambda)^{\frac{1}{2}} \operatorname{erf}(\lambda\tau)^{\frac{1}{2}} - \sum_{n=1}^{\infty} u_n'(0)(2Pr\lambda)^{-n/2} \left[\Gamma_{\lambda\tau}\left(\frac{n}{2}\right) \Big/ \Gamma\left(\frac{n}{2}\right)\right] \qquad (28)$$

$$G_0 = g_1 + g_2, \qquad G_1 = g_1 - g_2$$
$$G_2 = G_0 - g_3, \qquad G_3 = G_1 + (2Pr\lambda)^{\frac{1}{2}}\eta g_3 - g_4$$
$$G_4 = G_0 - (1 + \lambda\tau + Pr\lambda\eta^2) g_3 + \tfrac{1}{2}(2Pr\lambda)^{\frac{1}{2}}\eta g_4$$
$$G_5 = G_1 + (2Pr\lambda)^{\frac{1}{2}}\left(1 + \lambda\tau + \frac{Pr}{3}\lambda\eta^2\right)\eta g_3 - \left(1 + \frac{2}{3}\lambda\tau + \frac{Pr}{3}\lambda\eta^2\right) g_4, \text{ etc.}$$

* We have also evaluated u_3 and u_4; they are omitted from the list in order to conserve space. It has been found that five terms of the series are capable of providing satisfactory results for all cases considered.

with

$$\left.\begin{aligned} g_1 &= \tfrac{1}{2}\,\mathrm{erfc}\,[Pr^{\frac{1}{2}}(2\tau)^{-\frac{1}{2}}\eta - (\lambda\tau)^{\frac{1}{2}}] \\ g_2 &= \tfrac{1}{2}\{\exp[2(2Pr\lambda)^{\frac{1}{2}}\eta]\}\,\mathrm{erfc}\,[Pr^{\frac{1}{2}}(2\tau)^{-\frac{1}{2}}\eta + (\lambda\tau)^{\frac{1}{2}}] \\ g_3 &= \{\exp[(2Pr\lambda)^{\frac{1}{2}}\eta - \lambda\tau]\}\,\mathrm{erfc}\,[Pr^{\frac{1}{2}}(2\tau)^{-\frac{1}{2}}\eta] \\ g_4 &= 2\pi^{-\frac{1}{2}}(\lambda\tau)^{\frac{1}{2}}\exp\{-[Pr^{\frac{1}{2}}(2\tau)^{-\frac{1}{2}}\eta - (\lambda\tau)^{\frac{1}{2}}]^2\}. \end{aligned}\right\} \quad (25)$$

in which

$$\left.\begin{aligned} u_1'(0) &= Pr\lambda, \qquad u_2'(0) = \frac{aPr}{8}(1-2\beta) \\ u_3'(0) &= -\frac{Pr}{16}\beta(2-3\beta) + \frac{1}{2}Pr^2\lambda^2, \\ u_4'(0) &= \frac{aPr^2}{4}(1-2\beta)\,\lambda \end{aligned}\right\} \quad (28a)$$

etc.

The steady state temperature derivative at the wedge surface is

$$-\theta_s'(0) = (2Pr\lambda)^{\frac{1}{2}} - \sum_{n=1}^{\infty} u_n'(0)(2Pr\lambda)^{-n/2}. \quad (29)$$

Obviously, in both (28) and (29), λ implies $\lambda(0)$. The local transient surface flux is

$$q_w = -k(T_w - T_\infty)\left(\frac{m+1}{2}\frac{U}{\nu x}\right)^{\frac{1}{2}}\theta'(0,\tau) \quad (30)$$

and the corresponding Nusselt number is

$$Nu = \frac{q_w x}{(T_w - T_\infty)k} = -\left(\frac{m+1}{2}\right)^{\frac{1}{2}} Re^{\frac{1}{2}}\theta'(0,\tau). \quad (31)$$

4.1. *Steady-state solution and evaluation of* λ

To evaluate the function $\lambda(\eta)$, we must *separately* determine the steady state temperature field $\theta_s(\eta)$. It is well known that θ_s satisfies $\theta_s'' + Pr f\theta_s' = 0$, with $\theta_s(0) = 1$ and $\theta_s(\infty) = 0$. A number of investigators have reported results using different solution methods. They are well documented in the literature. For our purpose, it is most convenient to use once again the step-by-step calculation scheme mentioned earlier. The pertinent dimensionless wall derivative values were taken from [3]. Eckert [6] reported data of $\theta_s(\eta)$ to the fourth decimal place for $Pr = 0{\cdot}7$, 1·0 and 10 and for $\beta = -0{\cdot}14$, 0, 0·2, 0·5, 1·0 and 1·6. When our results were compared with his for the common values of Pr and β, complete agreement (up to and including the fourth decimal place) was observed for $Pr = 1$. However, some minor discrepancies in the last digit were noted for $Pr = 10$.

The numerical data so obtained for $\theta_s(\eta)$ were then inserted in (27) and $\lambda(\eta)$ determined therefrom. An iterative computer program was written for this purpose. The series in (27) is semi-divergent and Euler's transformation was used in the evaluation of the sum. While, in

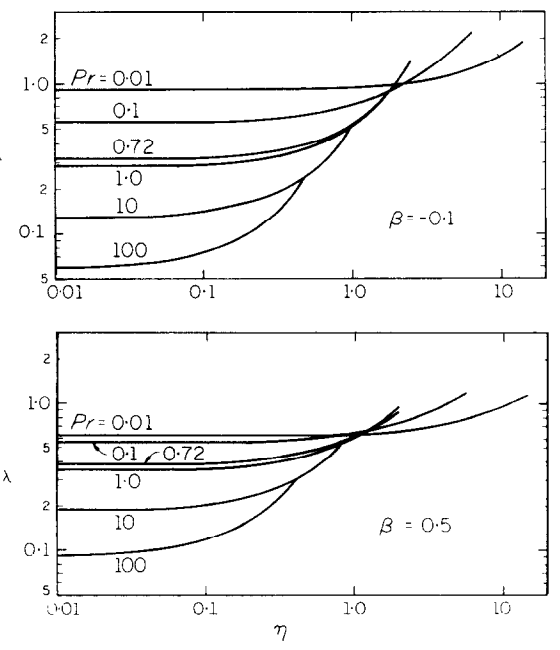

FIG. 2. Variation of $\lambda(\eta)$ with Prandtl number ($\beta = -0{\cdot}1, 0{\cdot}5$).

theory, the transformation can be initiated from any term, the most satisfactory result is achieved by choosing a starting point which would result in the best convergent sequence (in the Euler sense) and the smallest last term, with the least number of transformations.* When $\eta = 0$ the series in (27) becomes identically unity and hence it cannot be used to determine $\lambda(0)$. The latter was evaluated from (29) using the appropriate values of $-\theta_s'(0)$ taken from [3]. Data for all cases of Pr and β selected in this study may be found in [4]. To illustrate the general behavior of $\lambda(\eta)$, we present Fig. 2 which is for $\beta = -0{\cdot}1$ and 0·5. All plots exhibit the same feature that, at small η, λ is nearly a constant and it increases rather sharply as the edge of the thermal layer is approached.

Our computer program, in its final form, evaluates $f(\eta)$, $\theta_s(\eta)$, $X_n(\eta)$ and hence $u_n(\eta)$ for $n = 1, 2, 3$ and 4, $\lambda(\eta)$, $\theta(\eta, \tau)$ and the wall flux ratio $q_w/q_{w,s}$ in a single operation. Data were generated from an IBM 360 computer for the six Prandtl numbers and the six wedge angles with step sizes of η identical to those used for f. Transient temperature fields were calculated for $\tau = 0{\cdot}01$, 0·1 and 1·0. Wall fluxes were determined for τ ranging from 0·001 to 5 for $Pr = 0{\cdot}01$ and from 0·001 to 40 for $Pr = 100$. The total computer time was 80s†. If $\theta(\eta, \tau)$ and $q_w/q_{w,s}$ were excluded in the computation, the machine time was 52s.

4.2 *Transient temperature fields*

With the evaluation of λ, the transient temperature field in the boundary layer becomes completely determined and is given by (24). Likewise, the transient wall flux is given by (28) and (30). It should be noted that the series involved are not convergent. Because of the procedure used in the determination of $\lambda(\eta)$, each necessarily possesses a limit. This may be seen by comparing (24) with (27) and (28) with (29). Like G_n, the ratio $\Gamma_{\lambda\tau}(n/2)/\Gamma(n/2)$ in (28) is confined between 0 and 1. We may thus anticipate that the series in question are semi-divergent and Euler transformation was used in the evaluation of their sum. It has been consistently noted that best results are obtained when the transformation is applied in precisely the same manner as that used in the evaluation of λ.

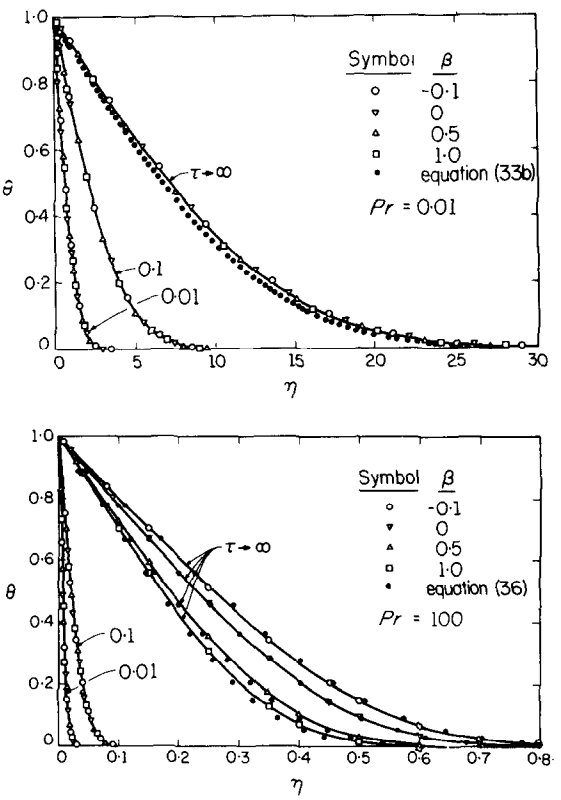

FIG. 3. Temperature fields following a step change in wedge surface temperature (a) for $Pr = 0{\cdot}01$, (b) for $Pr = 100$.

Extensive transient temperature field data have been tabulated in [5]. The highlights of the results are graphically displayed in Figs. 3a and 3b, respectively, for $Pr = 0{\cdot}01$ and 100. The manner by which the thermal layer grows

* Failure of strict adherence to this rule has resulted in errors in the values of $\lambda(0)$ reported in [1]. Consequently, the wall flux response shown in Fig. 2 of the said reference depicts somewhat too fast an approach to the steady state value.

† The corresponding time for the case of a step change in wall flux was 75 s.

with time is clearly seen. When $Pr = 0{\cdot}01$,* the dimensionless temperature distributions shown in Fig. 3a exhibit virtually no influence of β. This is to be expected during early times since, then, the heat-transfer process is governed by molecular diffusion. However, it is somewhat surprising to find that the data for different β's fall on a single curve within the thickness of the line even when the steady condition has been re-established. A possible physical explanation is that, when this occurs, the velocity boundary layer is completely submerged within a small fraction of the thermal layer in fluid of $Pr = 0{\cdot}01$. To further examine the nature of the *steady* temperature field in small Prandtl number fluids, we consider the limiting case of $Pr \to 0$. As has been pointed out in [7], under such circumstance we may neglect altogether the existence of the velocity boundary layer and replace the velocity components (u, v) in the energy equation by the following.

$$u \simeq U(x) = Cx^m$$

$$v \simeq -\frac{dU}{dx}y = -Cmx^{m-1}y. \tag{32}$$

It is simple to demonstrate that the solution, satisfying the boundary conditions $T(x, 0) = T_w$ and $T(x, \infty) = T_\infty$ is

$$\frac{T - T_\infty}{T_w - T_\infty} = \text{erfc}\left[\left(\frac{Pr}{2}\right)^{\frac{1}{2}}\left(\frac{m+1}{2}\frac{U}{vx}\right)^{\frac{1}{2}}y\right]. \tag{33a}$$

Or, equivalently,

$$\theta_s = \text{erfc}\left[\left(\frac{Pr}{2}\right)^{\frac{1}{2}}\eta\right], \qquad \text{for } Pr \to 0. \tag{33b}$$

In this limiting case, the temperature field is expressible in terms of a single variable, $(Pr/2)^{\frac{1}{2}}\eta$ which does not involve ν. In Fig. 3a, (33b) is shown plotted as filled circles. Their agreement with data obtained from the present analysis for $Pr = 0{\cdot}01$ is quite good. The local Nusselt number corresponding to (33b) is

$$Nu_s = \left(\frac{m+1}{\pi}\right)^{\frac{1}{2}} Re^{\frac{1}{2}}Pr^{\frac{1}{2}}, \qquad \text{for } Pr \to 0. \tag{34}$$

When $Pr = 100$, the dimensionless temperature distributions for various β's remain to lie in a single curve at small times but, as the steady state is approached, the influence of β is clearly revealed. The two distributions in accelerated flow ($\beta = 0{\cdot}5$ and $1{\cdot}0$) shown in Fig. 3b lie below that for the flat plate ($\beta = 0$) since a higher fluid acceleration facilitates convective transport and thus results in a steeper temperature gradient at the wall.

When the thermal layer is confined within a small fraction of the velocity boundary layer, as is the case for large Pr, the velocity field may be approximated by

$$\left.\begin{aligned} u &\simeq \frac{\tau_w(x)}{\mu}y \\ v &\simeq -\frac{1}{2\mu}\frac{d\tau_w}{dx}y^2 \end{aligned}\right\} \tag{35}$$

where τ_w is the local shear stress at wall. With this approximation, the solution of the *steady* state energy equation satisfying the simple boundary conditions previously stated has been discussed by Kestin and Persen [8]. Re-writing their result in terms of the present nomenclature gives

$$\theta_s = 1 - \frac{\Gamma_\zeta(\frac{1}{3})}{\Gamma(\frac{1}{3})}, \qquad \text{for large } Pr \tag{36}$$

where $\zeta = (aPr/6)\eta^3$ and $a = f''(0)$. Data calculated from (36) using the values of a listed in [3] are plotted as filled circles in Fig. 3b for the four β's shown. They agree well with the more precise distribution, particularly when $\beta = 0$. This is so because a sizable portion of the Blasius profile adjacent to the wall is very nearly linear. In flows with pressure gradient, either adverse or favorable, the linear approximation becomes poorer.

* All steady state or long time results reported in this paper for $Pr = 0{\cdot}01$ should be interpreted with caution. The boundary layer approximation which is implicit in (9) may become poor.

The local Nusselt number corresponding to (36) is

$$Nu_s = 0{\cdot}4358a^{\frac{1}{2}}(m+1)^{\frac{1}{2}}\,Re^{\frac{1}{2}}\,Pr^{\frac{1}{2}}, \quad \text{for large } Pr. \qquad (37)$$

The numerical constant is the equivalence of $3^{\frac{1}{2}} \cdot 2^{-\frac{1}{2}}/\Gamma(1/3)$. To ascertain the usefulness of (37), Table 1 is prepared.

at T_w for $t > 0$. In this case, the transient temperature field is

$$\theta = \operatorname{erfc}\left[\frac{y}{2(\kappa t)^{\frac{1}{2}}}\right] = \operatorname{erfc}\left[\eta\left(\frac{Pr}{2\tau}\right)^{\frac{1}{2}}\right]. \qquad (38)$$

Equation (38) suggests that, for sufficiently small times, the appropriate variable of the problem is $Pr^{\frac{1}{2}}\,\eta\tau^{-\frac{1}{2}}$. In Fig. 4, data evaluated from the

Table 1. *Values of* $\mathrm{Nu}_s\,\mathrm{Re}^{-\frac{1}{2}}\,\mathrm{Pr}^{-\frac{1}{2}}$ *calculated from the approximate formula* (37) *and those from present analysis*

β		−0·1	0	0·1	0·2	0·5	1·0
Approx. for large Pr		0·2908	0·3388	0·3744	0·4051	0·4907	0·6608
More exact analysis	$Pr = 100$	0·2948	0·3386	0·3717	0·4005	0·4814	0·6434
	$Pr = 10$	0·2987	0·3380	0·3681	0·3945	0·4695	0·6214
	$Pr = 1$	0·3014	0·3321	0·3562	0·3776	0·4400	0·5705

It is seen that (37) represents a good approximation even for moderate Prandtl numbers, especially when $\beta = 0$.

Within a short duration subsequent to the initiation of the thermal disturbance, the growth of the boundary layer is dominated by molecular diffusion. Hence, one might expect that, under this condition, the temperature field in the boundary layer would differ little from that in a semi-infinite *stationary* medium initially at a uniform temperature T_∞ and its surface temperature is suddenly brought up to and maintained

current analysis for the two extreme Prandtl numbers and for $\beta = -0{\cdot}1$, 0, 1·0 and $\tau = 0{\cdot}01$, 1·0 are compared with (38). At $\tau = 0{\cdot}01$, all data points fall on or very close to the pure conduction solution. When τ reaches 1·0, data for $Pr = 0{\cdot}01$ deviate significantly from the curve for all three β's. As expected, the largest deviation occurs in accelerated flow due to the relatively greater convection effects. On the other hand, data for $Pr = 100$ remain quite close to the conduction solution when $\tau = 1{\cdot}0$, particularly for $\beta = -0{\cdot}1$ and 0. This means that the

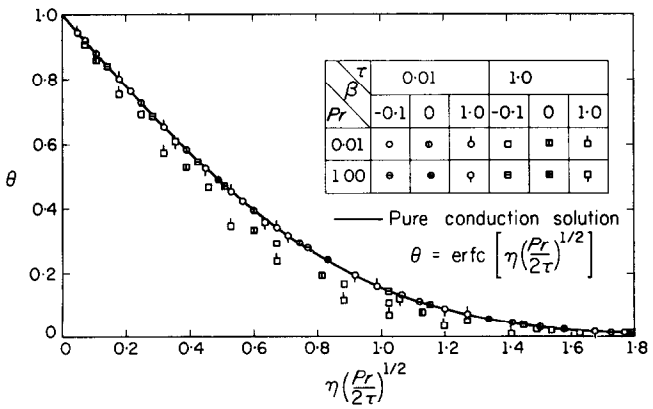

FIG. 4. Comparison of transient temperature fields with pure conduction solution.

numerical value of τ beyond which the transient behavior is no longer controlled by molecular diffusion process depends on the Prandtl number of the fluid. This value is higher for higher Pr and, for a given Pr, it is somewhat less for larger β.

4.3 *Transient wall flux response*

In engineering design applications, it often is convenient to describe the wall flux response in terms of the ratio of its instantaneous value to the steady state value, namely, $q_w/q_{w,s}$ or, equivalently, Nu/Nu_s. This ratio may be determined by dividing $\theta'(0,\tau)$ by $\theta'_s(0)$. The former is given by (28) and the latter is available from [3]. Extensive results for all combinations of β and Pr have been tabulated in [4]. When they are plotted against τ on log–log coordinates, the resulting curves all bear a resemblance to those shown in Fig. 2 of [1], which is for $\beta = 0$. For a fixed Pr, increasing β displaces the curves downward. This effect is most pronounced for $Pr = 100$ and gradually diminishes with decreasing Pr. When $Pr = 0{\cdot}01$, the said effect becomes insignificant.

The calculated wall flux ratio data, $q_w/q_{w.s}$, for all 36 combinations of β and Pr can be correlated in a manner similar to that illustrated in Fig. 3 of [1] by using an empirically defined time parameter of the form:

$$[B(Pr,\beta)]\, Pr^{-b(\beta)}\,\tau.$$

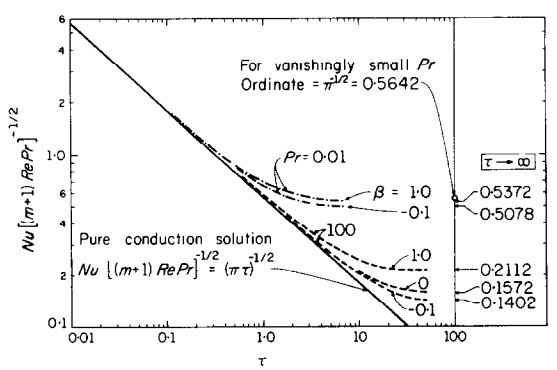

FIG. 5. Departure of surface heat flow from pure conduction transient.

Details may be found in [4]. Here we merely mention that b decreases approximately linearly with increase in β, being $\frac{1}{3}$ for $\beta = 0$ and $\frac{1}{4}$ for $\beta = 1$. When Pr is within the range of 0·72 and 100, B becomes essentially a function of β alone.

An expression for small time whose validity extends beyond that of the pure conduction transient can be readily obtained by introducing the appropriate series expansions for the exponential, error, and incomplete gamma functions in (28). Substituting the result in (31) and rearranging give

$$Nu[(m+1)\,RePr]^{-\frac{1}{2}} = (\pi\tau)^{-\frac{1}{2}} + 0 + 0 - \frac{a}{16}(2Pr)^{-\frac{1}{2}}(1-2\beta)\,\tau + \frac{1}{48\sqrt{\pi}}\,Pr^{-1}\,\beta(2-3\beta)\,\tau^{\frac{3}{2}} + \ldots \qquad (39)$$

The first term on the right-hand side corresponds to the conduction transient. It is interesting to note that, for the several terms shown in (39), λ does not appear. Similar behavior has previously been reported [1, 2].

With the results available from this study, it is easy to ascertain the time beyond which the wall flux response would significantly deviate from the conduction transient and the manner by which Pr and β would influence such time. This information is provided in Fig. 5. To a large extent, the figure is self-explanatory. The numerals shown under the box inscribed with $\tau \to \infty$ refer to the steady state values of $Nu[(m+1)\,RePr]^{-\frac{1}{2}}$ for the several Pr's and β's indicated.

5. RESULTS FOR A STEP CHANGE IN WALL FLUX

Since the procedure used is completely analogous to that described in Section 4, we shall refrain from presenting the details of the derivation. Interested readers may consult [4].

5.1 *Steady state solution*

For the problem under consideration, the steady state temperature field satisfies

$$\theta_s'' + Prf\theta_s' = (1-\beta)\,Prf'\theta_s \qquad (40)$$

with

$$\theta_s'(0) = -1, \qquad \theta_s(\infty) = 0 \tag{41}$$

and θ_s is defined by (13b) with T being time-independent. Unlike the case of uniform wall temperature, the solution has not been extensively reported except for $\beta = 0$ and 1·0. Complete data for the profiles are available in [4]. Table 2 lists the wall values. At first glance, the data appear to lack uniformity. For $Pr = 0{\cdot}01$, the dimensionless wall temperature function $\theta_s(0)$ increases monotonically with β. For the remaining five Pr's, it first decreases with increasing β, reaches a minimum and then increases with further increase in β. The percentage variation is the least for $Pr = 100$. A more close examination reveals that the said minimum occurs at a value of β which decreases with decreasing Prandtl number. For $Pr = 0{\cdot}01$, this minimum is beyond the smallest $\beta(-0{\cdot}1)$ investigated and thus disappears in Table 2.

Table 2. Values of $\theta_s(0) \equiv \theta_{w,s}$

Pr \ β	−0·1	0	0·1	0·2	0·5	1·0
0·01	9·09098	9·11709	9·24913	9·44376	10·32660	13·16270
0·10	3·62785	3·52401	3·50154	3·51932	3·72022	4·55579
0·72	1·83015	1·72519	1·68143	1·66514	1·70266	1·99428
1·0	1·64137	1·54064	1·49758	1·48009	1·50651	1·75295
10·0	0·77194	0·70861	0·67990	0·66551	0·66285	0·74690
100·0	0·36219	0·32859	0·31333	0·30537	0·30127	0·33469

With the availability of $\theta_s(\eta)$, $\lambda(\eta)$ can be determined. Their general behavior is similar to those shown in Fig. 2.

5.2 *Transient temperature fields*

Figures 6a and 6b show the calculated results for the two extreme Prandtl numbers. At sufficiently small times, data for different β's fall closely on a single curve, again manifesting the dominance of molecular diffusion. For $Pr = 0{\cdot}01$, the influence of β is clearly discernible when $\tau = 1$.* For higher Prandtl number fluids, this effect of fluid acceleration will not be felt until greater values of τ are reached. Due to the imposed flux condition at wall, all curves have identical slope at $\eta = 0$. In comparing these results with those illustrated in Figs. 3a and 3b, one should be reminded of the basic difference in the definition of θ for the two cases.

We have also separately examined the steady state solution for vanishingly small Pr and for large Pr† when the wall flux is uniform. It has been found that, in either case, similar solutions exist. However, unlike the case of uniform wall temperature, a plot of θ_s vs. η for $Pr \to 0$ would exhibit different curves for different β's. Furthermore, attempts to obtain closed form solutions failed, except for the following cases.

(a) For $Pr \to 0$

(a.1) Flat plate, $\beta = 0$.

Here $U = U_\infty$ and $\eta = y[(U_\infty)/(2\nu x)]^{\frac{1}{2}}$.

Hence

$$\theta_s \equiv \frac{T - T_\infty}{\frac{q_w}{k}\left(\frac{2\nu x}{U_\infty}\right)^{\frac{1}{2}}} = \left(\frac{2}{Pr}\right)^{\frac{1}{2}} \cdot \text{ierfc}\left[\left(\frac{Pr}{2}\right)^{\frac{1}{2}}\eta\right] \tag{42}$$

and

$$\theta_{w,s} = \left(\frac{2}{\pi Pr}\right)^{\frac{1}{2}}. \tag{43}$$

* For clarity, data for $\beta = 0{\cdot}5$ are left unconnected.

† In the sense that a linear, longitudinal velocity distribution is a valid approximation.

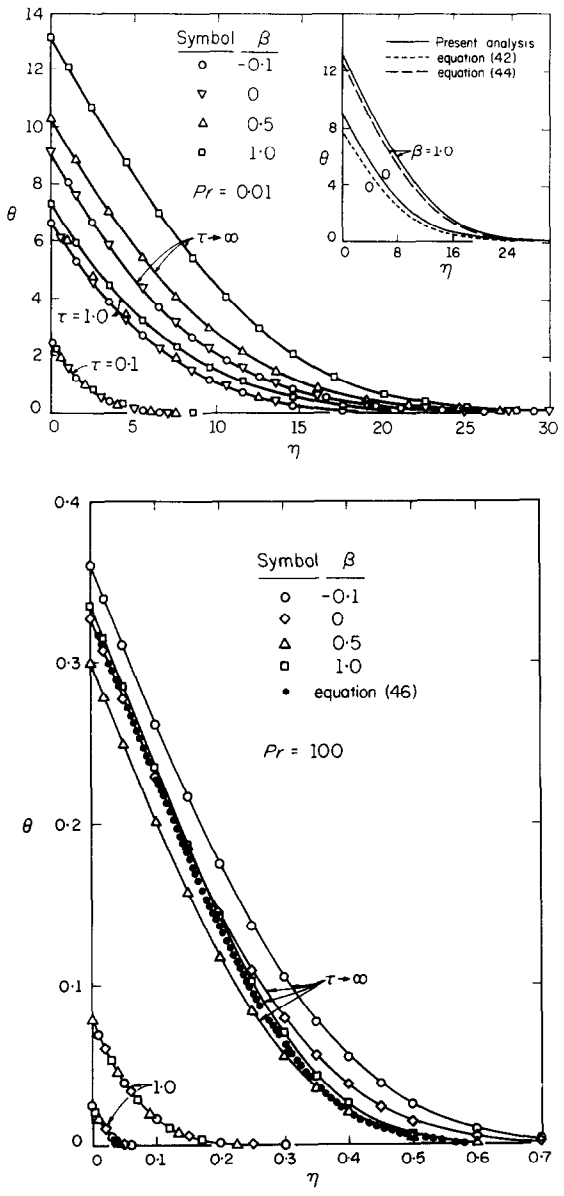

FIG. 6. Temperature fields following a step change in wedge surface flux (a) for $Pr = 0{\cdot}01$, (b) for $Pr = 100$.

(a.2) Forward stagnation, $\beta = 1$.

Here $U = Cx$, and $\eta = y(C/\nu)^{\frac{1}{2}}$. Thus

$$\theta_s = \frac{T - T_\infty}{\frac{q_w}{k}\left(\frac{\nu}{C}\right)^{\frac{1}{2}}} = \left(\frac{\pi}{2Pr}\right)^{\frac{1}{2}} \operatorname{erfc}\left[\left(\frac{Pr}{2}\right)^{\frac{1}{2}}\eta\right] \quad (44)$$

and

$$\theta_{w,s} = \left(\frac{\pi}{2Pr}\right)^{\frac{1}{2}}. \quad (45)$$

(b) For large Pr.

The only closed form solution found has been for the forward stagnation, $\beta = 1$. It is

$$\theta_s = \frac{T - T_\infty}{\frac{q_w}{k}\left(\frac{\nu}{C}\right)^{\frac{1}{2}}} = \left(\frac{6}{aPr}\right)^{\frac{1}{3}} \frac{\Gamma(\frac{1}{3})}{3}\left[1 - \frac{\Gamma_\zeta(\frac{1}{3})}{\Gamma(\frac{1}{3})}\right] \quad (46)$$

where $a = f''(0) = 1{\cdot}23259$ and $\zeta = (aPr/6)\eta^3$. The wall temperature is uniform and is given by

$$\theta_{w,s} = \frac{T_w - T_\infty}{\frac{q_w}{k}\left(\frac{\nu}{C}\right)^{\frac{1}{2}}} = 1{\cdot}513\, Pr^{-\frac{1}{3}}. \quad (47)$$

It is interesting to note that $\theta_{w,s} \sim Pr^{-\frac{1}{2}}$ when $Pr \to 0$ and $\theta_{w,s} \sim Pr^{-\frac{1}{3}}$ for large Pr.

Equations (42) and (44) have been plotted and are shown in the insert of Fig. 6a. The data obtained from these equations fall below those of the corresponding exact solution. The discrepancy is, of course, due to the complete neglect of the velocity boundary layer in the limiting analysis. Equation (46) is shown in Fig. 6b by the filled circles.

As in the previous case, the pure conduction solution would be a valid approximation immediately after the wall flux disturbance. It is given by

$$T - T_\infty = \frac{q_w}{k} 2(\kappa t)^{\frac{1}{2}} \operatorname{ierfc}\frac{y}{2(\kappa t)^{\frac{1}{2}}} \quad (48a)$$

which, when re-expressed in terms of the dimensionless variables used in the present study, becomes

$$\theta \equiv \frac{T_w - T_\infty}{\frac{q_w}{k}\left(\frac{2}{m+1}\frac{\nu x}{U}\right)^{\frac{1}{2}}} = \left(\frac{2\tau}{Pr}\right)^{\frac{1}{2}} \operatorname{ierfc}\left[\left(\frac{Pr}{2\tau}\right)^{\frac{1}{2}}\eta\right]. \quad (48b)$$

In Fig. 7, a comparison is made with the presently calculated data for $\beta = -0{\cdot}1$, 0 and 1·0 and for several combinations of Pr and τ giving rise

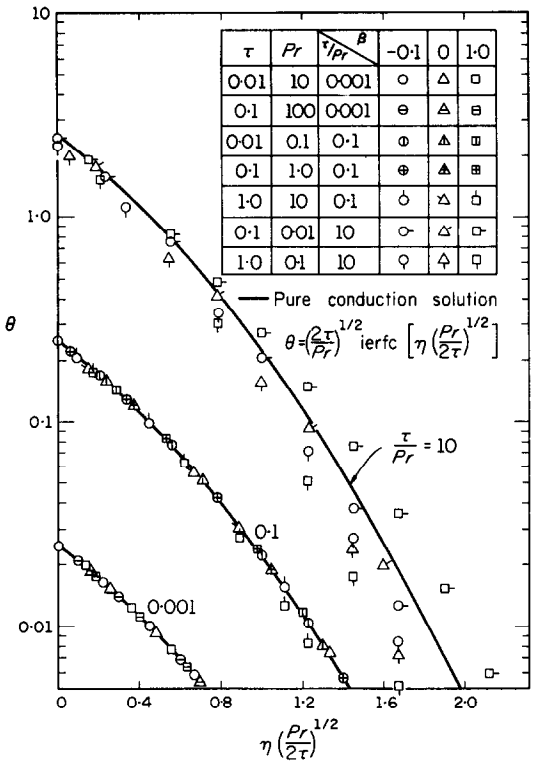

FIG. 7. Comparison of transient temperature fields with pure conduction solution.

to $\tau/Pr = 10^{-3}, 10^{-1}$ and 10. When $\tau/Pr = 10^{-3}$, the agreement is very good manifesting that the heat transfer process closely follows that due to molecular diffusion alone. When $\tau/Pr = 10^{-1}$, (48b) remains to show good agreement with the data, except for $\beta = 1{\cdot}0$. This indicates that the convective influence has come into play in the highly accelerated flow. When $\tau/Pr = 10$, the conduction solution ceases to be useful.

5.3 *Transient wall temperature response*

The general behavior of the wall temperature response expressed as a ratio $\theta_w/\theta_{w,s}$ and plotted against τ is similar to that displayed in Fig. 4 of [1]. For $Pr = 0{\cdot}01$, the effect of increasing β is to displace the curve downward, with the one for $\beta = -0{\cdot}1$ occupying the top position. For $Pr = 100$, the influence of changing β on the relative displacement of the curves becomes small. This is in contrast to the role which Pr plays in influencing the effect of β on the wall flux behavior subsequent to a step change in wall temperature. At present, a satisfactory physical explanation is lacking.

To illustrate the manner by which the response behavior deviates from the diffusion process as time proceeds and the extent to which β and Pr exert their influence, we include Fig. 8. Finally we note that it has also been found possible to correlate all wall temperature ratio data by defining an empirical time parameter similar to but modified from that used in the previous case. Again, for Pr ranging from 0·72 to 100, the response time varies as $Pr^{b(\beta)}$.

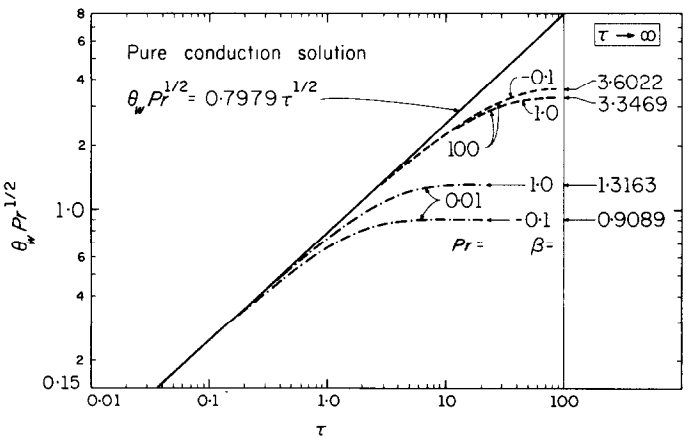

FIG. 8. Departure of wall temperature response from pure conduction transient.

ACKNOWLEDGEMENT

This research was supported in part by a National Science Foundation Grant GK-16270 of the U.S. Government.

REFERENCES

1. B. T. CHAO and L. S. CHEEMA, Unsteady heat transfer in laminar boundary layer over a flat plate, *Int. J. Heat Mass Transfer* **11**, 1311–1324 (1968).
2. B. T. CHAO and JAMES L. S. CHEN, Series solution of unsteady heat or mass transfer to a translating fluid sphere, *Int. J. Heat Mass Transfer* **13**, 359–367 (1970).
3. E. ELZY and R. M. SISSON, *Tables of Similar Solutions to the Equations of Momentum, Heat and Mass Transfer in Laminar Boundary Layer Flow*. Eng. Exp. Station Bulletin No. 40, Oregon State University, Corvallis, Oregon (1967).
4. J. L. S. CHEN, Thermal response behavior of laminar boundary layers in wedge flow, Ph.D. thesis, University of Illinois at Urbana-Champaign (1969).
5. L. ROSENHEAD (editor), *Laminar Boundary Layers*, Table V.1, p. 224, Table V.2, p. 232; and Table V.3, p. 237. Oxford University Press (1963).
6. E. R. G. ECKERT, Die Berechnung des Wärmeüberganges in der Laminar Grenzschicht umströmter Körper, *VDI-Forschungsheft* 416, (1942).
7. H. SCHLICHTING, *Boundary-Layer Theory*, 6th edn., p. 271. McGraw-Hill, New York (1968).
8. J. KESTIN and L. N. PERSEN, The transfer of heat across a turbulent boundary layer at very high Prandtl numbers, *Int. J. Heat Mass Transfer* **5**, 355–371 (1962).

COMPORTEMENT DE LA RÉPONSE THERMIQUE DES COUCHES LIMITES LAMINAIRES DANS L'ÉCOULEMENT AUTOUR DE DIÈDRES

Résumé—Le comportement de la réponse thermique des écoulements de couche limite laminaire, incompressible et à propriétés uniformes sur des dièdres a été étudié en employant une technique proposée récemment par Chao et Cheema. On obtient les caractéristiques de la réponse de surface et les détails des champs transitoires de température, à la suite d'une variation en échelon, soit de la température, à la suite d'une variation en échelon, soit de la température de surface, soit du flux de chaleur à la surface. Les résultats sont présentés pour des nombres de Prandtl de 0,01, 0,1, 0,72, 1,0, 10 et 100 et pour des dièdres avec $\beta = -0{,}1, 0, 0{,}1, 0{,}2, 0{,}5$ et 1,0, $\pi\beta$ étant l'angle du dièdre. Une connaissance physique révélatrice est obtenue en comparant les résultats pour des temps faibles avec des transitoires de conduction pure et les résultats pour l'état permanent avec ceux déduits pour des nombres de Prandtl infiniment faibles et pour des nombres de Prandtl élevés.

VERHALTEN THERMISCHER SIGNALE IN LAMINAREN GRENZSCHICHTEN BEI KEILSTRÖMUNG

Zusammenfassung— Es wird Verhalten thermischer Signale in inkompressiblen, laminaren Grenzschichtströmungen konstanter Stoffeigenschaften über Keile untersucht, idem man ein kürzlich von Chao und Cheema vorgeschlagenes Verfahren benutzt. Sowohl die Charakteristiken von Oberflächensignalen als auch Einzelheiten der instationären Temperaturfelder als Folge einer sprunghalften Änderung entweder der Oberflächentemperatur oder des Wärmestromes durch die Oberfläche werden erhalten, Ergebnisse werden angegeben für Prandtl-Zahlen von 0,01; 0,1; 0,72; 1,0; 10 und 100 für Keile mit $\beta = -0{,}1; 0; 0{,}1; 0{,}2; 0{,}5$ und 1,0. π wobei β der Keilwinkel ist. Ein aufschlussbreicher physikalischer Einblick wird gewonnen, indem man die Daten für kleine Zeiten mit reiner instationärer Wärmeleitung und die stationären Daten mit jenen vergleicht, die für verschwindend kleine Prandtl-Zahlen und für grosse Prandtl-Zahlen abgeleitet sind.

ТЕПЛОВОЙ ЛАМИНАРНЫЙ ПОГРАНИЧНЫЙ СЛОЙ В КЛИНЕ

Аннотация—Исследуется тепловой ламинарный пограничный слой несжимаемой жидкости в клине, используя методику, недавно предложенную Чао и Чимом. Получены поверхностные характеристики и данные о нестационарных температурных полях, являющихся результатом ступенчатого изменения либо температуры стенки, либо теплового потока на поверхности. Результаты приводятся для чисел $Pr = 0{,}01; 0{,}1; 0{,}72; 1{,}0; 10$ и 100 и угла клина $\beta = -0{,}1; 0; 0{,}1; 0{,}2; 0{,}5$; и $1{,}0\,\pi\beta$. Физический смысл раскрывается путём сравнения данных для малых отрезков времени, включая данные для переходных и стационарных режимов с данными, выведенными для пренебрежимо малого и большого чисел Прандтля.